The anomalous photovoltaic effect based on molecular chirality: the influence of the enantiomer purity on the photocurrent response in π-conjugated ferroelectric liquid crystals

Atsushi Seki, Yusuke Funatsu and Masahiro Funahashi[*]

Department of Advanced Materials Science, Faculty of Engineering, Kagawa University,
2217-20 Hayashi-cho, Takamatsu, Kagawa, 761-0396, Japan.
E-mail: m-funa@eng.kagawa-u.ac.jp; Fax: (+81)-87-864-2411; Tel: (+81)-87-864-2411.
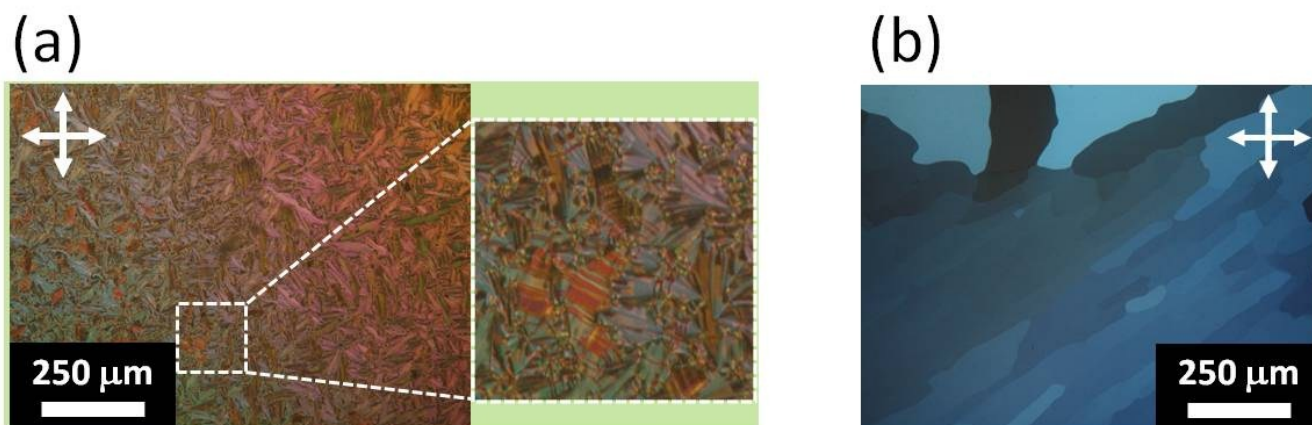
POM images of (*S*)-1

Figure S-1. POM images of (a) the SmC* phase (125 °C) and (b) the SmG* phase (50 °C) of (*S*)-**1** on cooling between two glass substrates. The inset is a magnified image of the SmC* phase at 125 °C. (These are magnified images of Figure 4.)

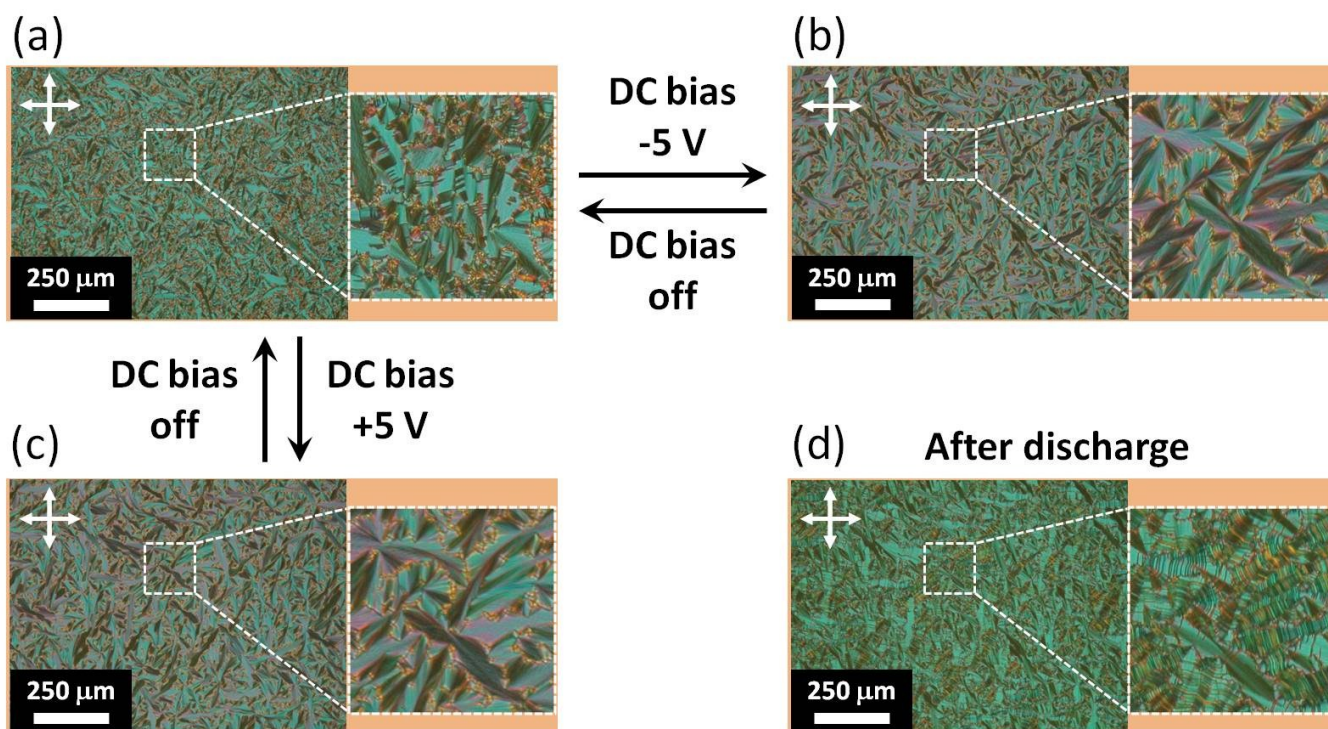**Molecular reorientation behaviors induced by electric field for (*S*)-1**

Figure S-2. POM images of the SmC* phase (127 °C) in a 2 μm-thick cell filled with (*S*)-**1**: (a) after cooling from the Iso phase without DC bias, (b) under application of a negative DC bias (-5 V), (c) under application of a positive DC bias (+5 V), and (d) after discharge. (These are magnified images of Figure 5.)
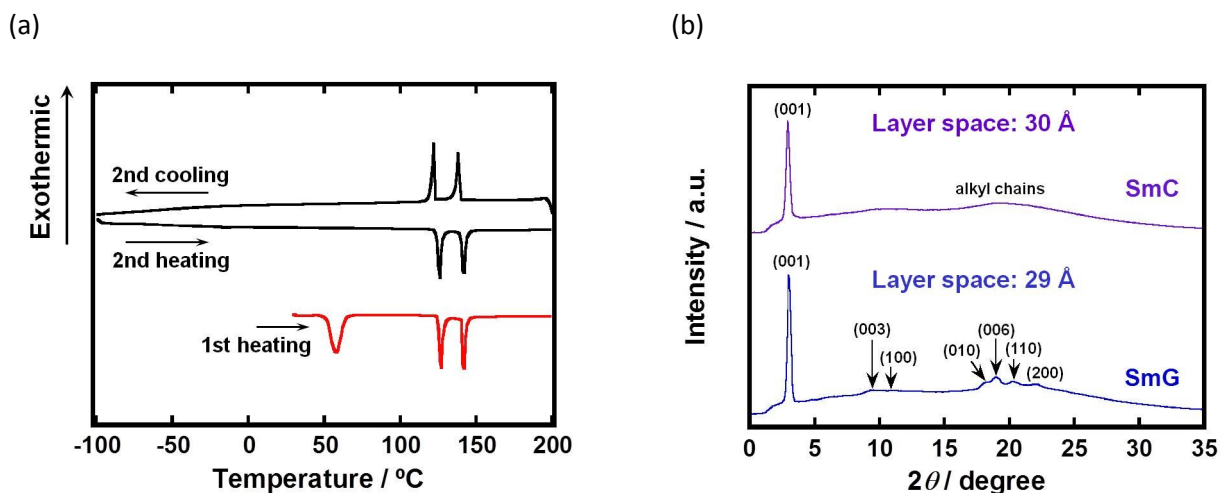
Characterization of mesomorphic properties for (*rac*)-1

Figure S-3. (a) DSC thermograms of (*rac*)-**1** (Scanning rates: 10 K/min. The red curves exhibit thermograms of obtained materials from recrystallization.); (b) XRD patterns in the LC phases of (*rac*)-**1** on cooling process (Upper: at 126 °C in the SmC phase, bottom: at 100 °C in the SmG phase).

Molecular reorientation behaviors induced by electric field for (*rac*)-1
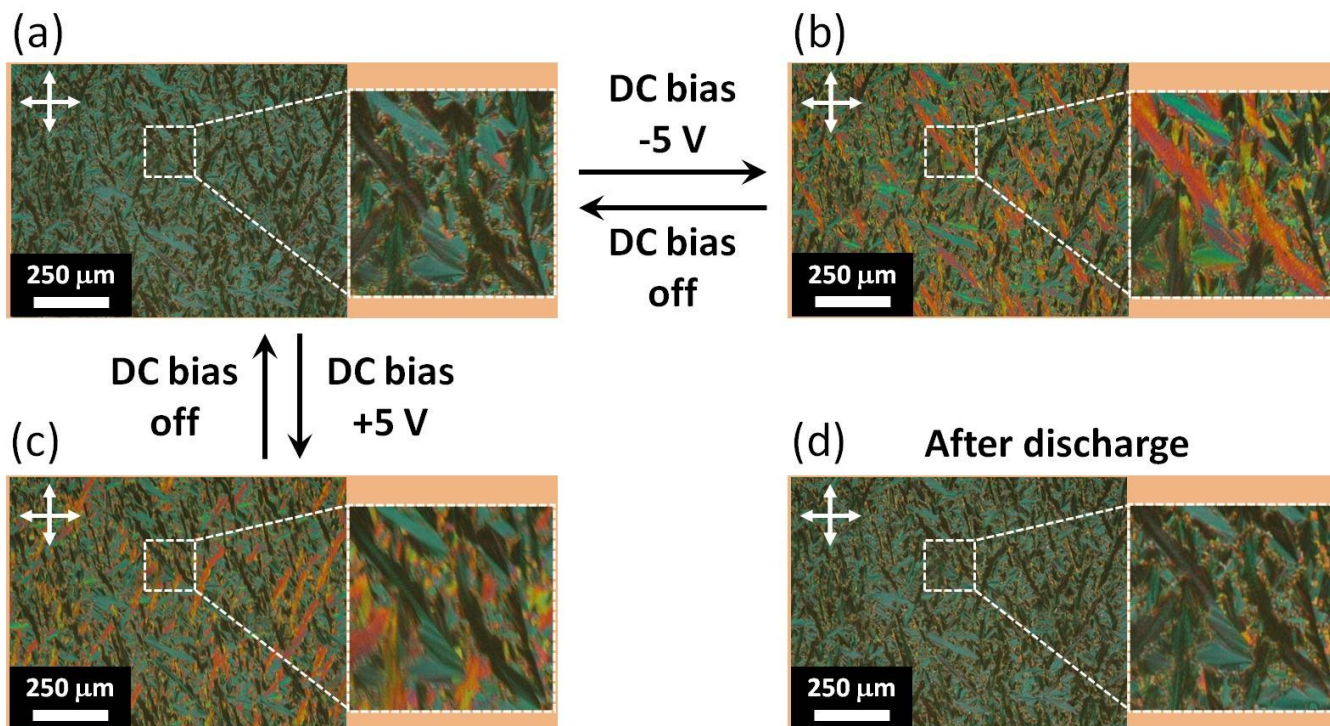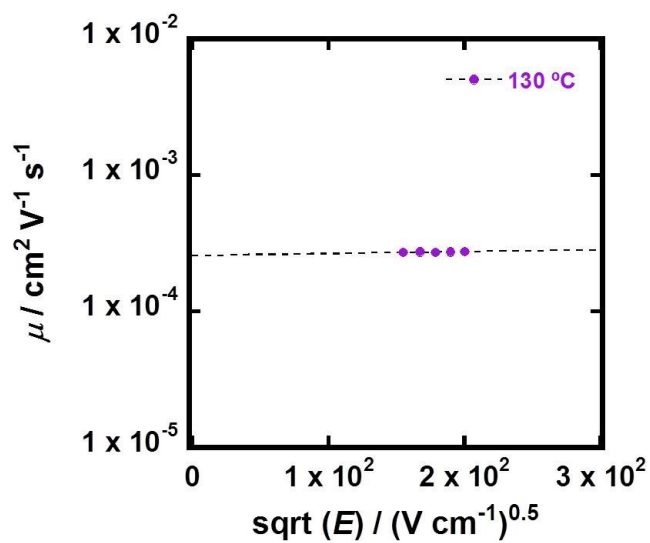

Figure S-4. POM images of the SmC phase (127 °C) in a 2-μm thick cell filled with (*rac*)-**1**: (a) after cooling from the Iso phase without DC bias, (b) under application of a negative DC bias (-5 V), (c) under application of a positive DC bias (+5 V), and (d) after discharge. (These are magnified images of Figure 8.)

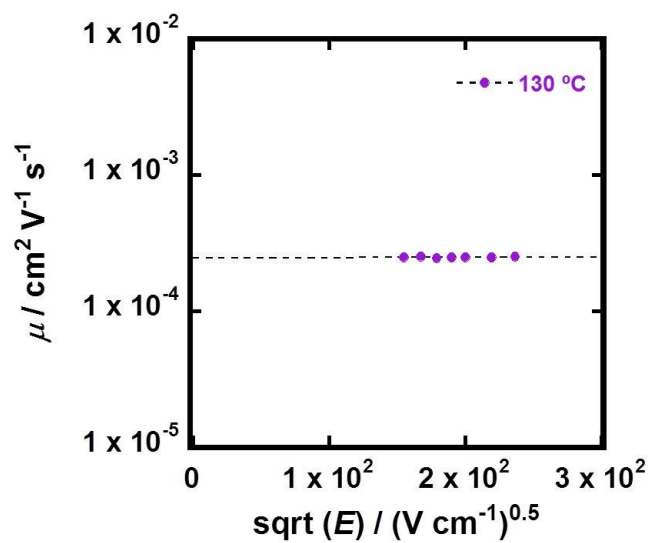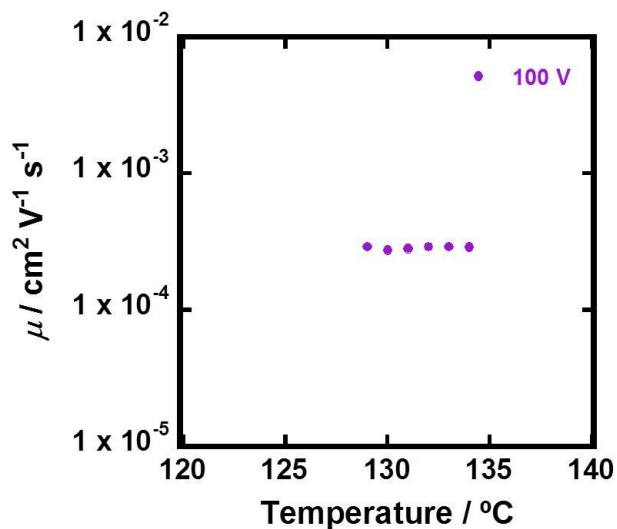**Electric-field-dependence of hole mobilities**

(a) (*S*)-**1**

(b) (*rac*)-**1**

Figure S-5. Hole mobilities as a function of the square root of electric field in (a) the SmC* phase of (*S*)-**1** and (b) the SmC phase of (*rac*)-**1**.

Temperature-dependence of hole mobilities

(a) (*S*)-**1**

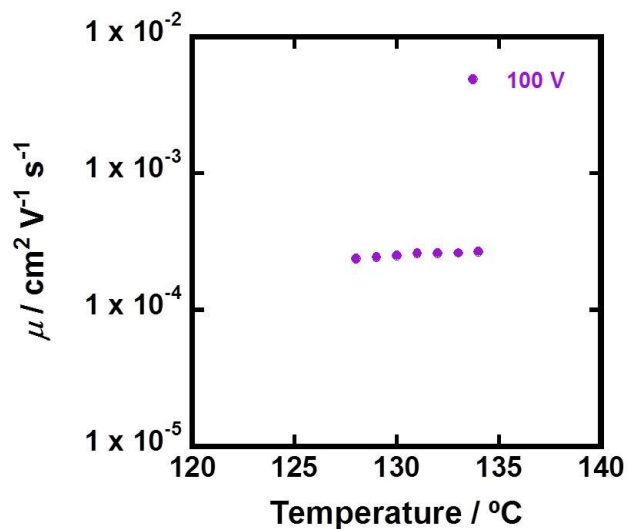(b) (*rac*)-**1**

Figure S-6. Hole mobilities as a function of temperature in (a) the SmC* phase of (*S*)-**1** and (b) the SmC phase of (*rac*)-**1**.

Frequency-dependence of dielectric hysteresis behavior in the SmC* phase of (*S*)-1
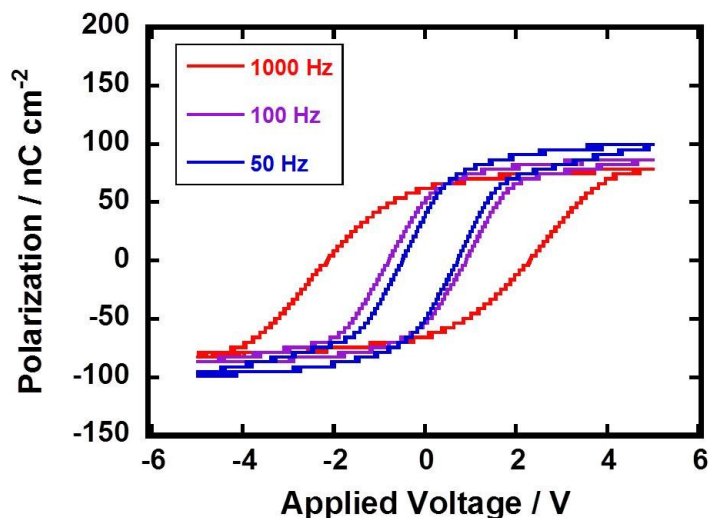

Figure S-7. Dielectric hysteresis loops in the SmC* (SmC) phase (130 °C) of (*S*)-**1**.

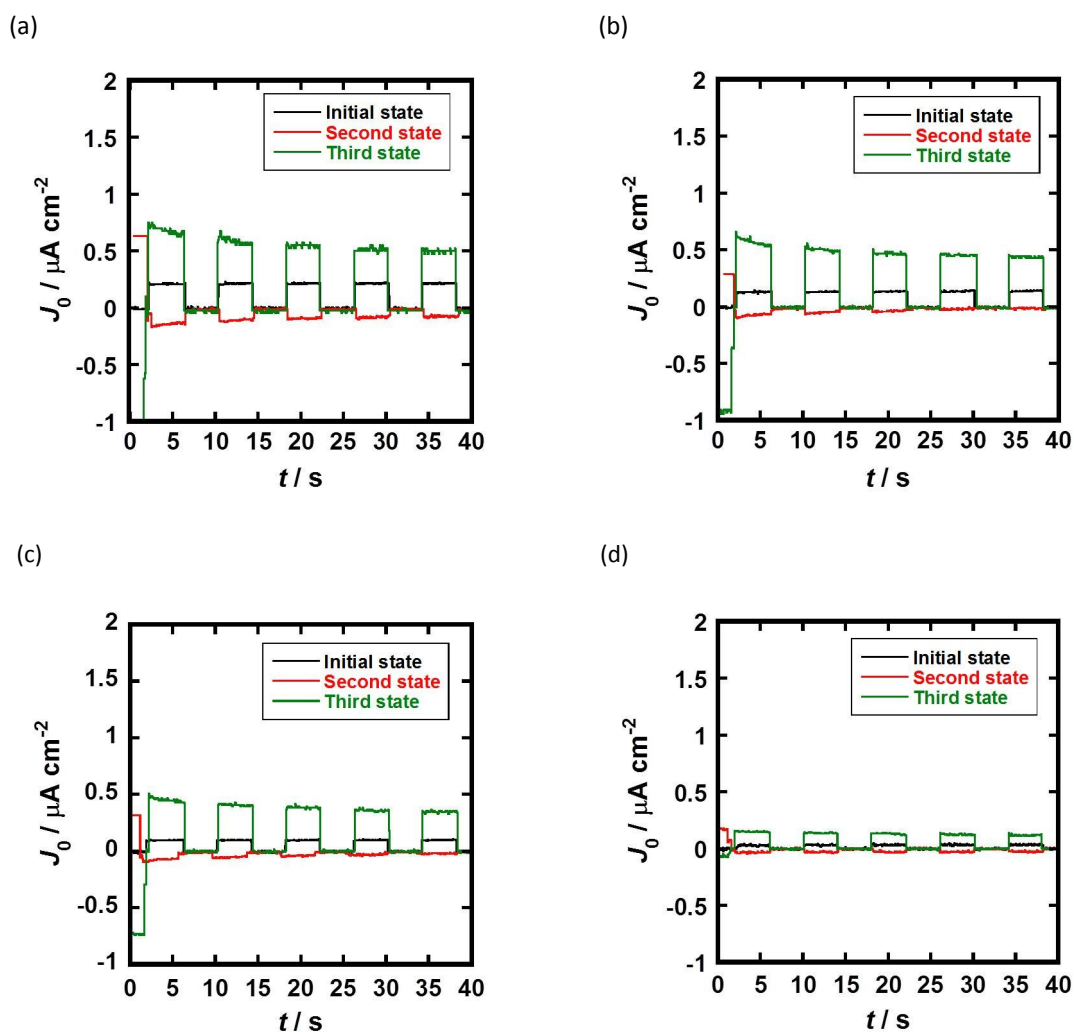**APV response of the 2-μm gap LC sample in their SmC*/SmC phases**

(a)

(b)

(c)

(d)

Figure S-8. Steady state photocurrent response profiles at 127 °C for (a) 1*R10S*-**1**, (b) 1*R6S*-**1**, (c) 1*R2S*-**1**, and (d) (*rac*)-**1**, (b) The measurements were performed using ITO/ ITO sandwich cells whose thickness was 2 μm. The APV current density (J_0) is determined as APV photocurrent density at zero external bias.